Available online at www.sciencedirect.com

SciVerse ScienceDirect

Solar Energy 86 (2012) 2620–2631

SOLAR ENERGY

www.elsevier.com/locate/solener

Three-dimensional thermal modeling of a photovoltaic module under varying conditions

M. Usama Siddiqui [a], A.F.M. Arif [a,*], Leah Kelley [b], Steven Dubowsky [b]

[a] Department of Mechanical Engineering, King Fahd University of Petroleum and Minerals, Dhahran 31261, Saudi Arabia
[b] Department of Mechanical Engineering, Massachusetts Institute of Technology, Cambridge, MA 02139, USA

Received 26 November 2011; received in revised form 11 May 2012; accepted 31 May 2012
Available online 14 July 2012

Communicated by: Associate Editor Igor Tyukhov

Abstract

Photovoltaic technology provides the direct method to convert solar energy into electricity. Modeling and simulation plays a very important role in the development of PV devices as well as in the design of PV systems. The objective of the current work was to develop a novel thermal model to simulate the thermal performance of PV modules with and without cooling. The model was sequentially coupled with a radiation model and an electrical model to calculate the electrical performance of the PV panels. Using the developed model, various studies were performed to evaluate the electrical and thermal performance of the module under different environmental and operating conditions with and without cooling. Results show that the performance of the PV panel with cooling had very little influence of increasing absorbed radiation (200–1000 W/m^2) at a constant ambient temperature (25 °C) and increasing ambient temperature (0–50 °C) at an absorbed radiation of 800 W/m^2. For the same variation in conditions, the performance of the panel without any cooling reduced significantly.

Keywords: Photovoltaic thermal collector; Simulation; PV cells; Finite element analysis

1. Introduction

Photovoltaic (PV) technology provides a direct method to convert solar energy into electricity. In recent years, the use of PV systems has increased greatly with many applications of PV devices in systems as small as battery chargers to large scale electricity generation systems and satellite power systems. At present, the conversion efficiency for commercial PV modules is between 13% and 20% (Armstrong and Hurley, 2010). The remaining solar energy absorbed into the panel is converted to heat and increases the panel temperature. Moreover, an increase in the module temperature causes the module efficiency to decrease (Skoplaki and Palyvos, 2009). Therefore, decreasing the cell temperature can lead to better conversion efficiency for the PV cells and thus to better PV system performance.

In order to improve PV electrical output and to collect additional energy in the form of hot water, Photovoltaic/thermal (PV/T) collectors of various designs have been developed. These collectors can either be custom-made PV/T collectors specially designed for thermal energy collection along with electricity generation or made from off-the-shelf PV panels being cooled by heat exchangers. Teo et al. (2011) designed and developed an air cooled PV/T system using a commercially available PV panel and a custom made air collector and found that the electrical efficiency of the PV panel was increased from 8.6% to 12.5% when the panel was cooled. Huang et al. (2001) presented the design of a water-type PV/T collector called the Integrated PhotoVoltaic Thermal System (IPVTS) and did

* Corresponding author.
E-mail address: afmarif@kfupm.edu.sa (A.F.M. Arif).

0038-092X/$ - see front matter © 2012 Elsevier Ltd. All rights reserved.
http://dx.doi.org/10.1016/j.solener.2012.05.034

Nomenclature

a	modified diode ideality factor
a_{ref}	modified diode ideality factor at STC
A_i	anisotropy index
A_{panel}	area of PV panel (m^2)
C_p	specific heat capacity (J/kg K)
C_μ, $C_{\varepsilon 1}$, $C_{\varepsilon 2}$	constants for turbulence model
E_g	band-gap energy of PV cell material (eV)
$E_{g,ref}$	band-gap energy of PV cell material at STC (eV)
$F_{front/rear\text{-}ground}$	geometric factor for front glass or back sheet to ground radiation
$F_{front/rear\text{-}sky}$	geometric factor for front glass or back sheet to sky radiation
G_b	horizontal beam radiation (W/m^2)
G_d	horizontal diffuse radiation (W/m^2)
G_{ref}	reference condition (STC) incident radiation (W/m^2)
h	heat loss coefficient (W/m^2 K)
$h_{conv,forced}$	forced convection coefficient (W/m^2 K)
$h_{conv,free}$	free convection coefficient (W/m^2 K)
$h_{radiation}$	radiation heat loss coefficient (W/m^2 K)
I	PV panel output current (A)
I_L	light generated current (A)
$I_{L,ref}$	light generated current at STC (A)
I_o	diode reverse saturation current (A)
$I_{o,ref}$	diode reverse saturation current at STC (A)
k_{cond}	thermal conductivity (W/m K)
k	turbulent kinetic energy (m^2/s^2)
K	extinction coefficient
$K_{\tau\alpha,b}$	incidence angle modifier for beam radiation
$K_{\tau\alpha,d}$	incidence angle modifier for diffuse radiation
$K_{\tau\alpha,g}$	incidence angle modifier for ground reflected radiation
L_{glass}	thickness of front glass layer (m)
m	irradiance dependence parameter for I_L
M	air mass modifier
n	temperature dependence parameter for a
$\boldsymbol{n}$	surface normal
NCS	number of PV cell in series in PV panel
Nu	Nusselt's number
P_k	Production term
Pr	Prandl's number
$\boldsymbol{q}$	heat conduction (W)
Q	volumetric heat generation (W/m^3)
Q_{vh}	viscous energy dissipation (W/m^3)
R_{beam}	geometric factor for beam radiation
Ra	Raleigh's number
Re	Reynolds's number
R_s	series resistance (Ω)
$R_{s,ref}$	series resistance at STC (Ω)
R_{sh}	shunt resistance (Ω)
$R_{sh,ref}$	shunt resistance at STC (Ω)
S	plane-of-array absorbed solar radiation at operating conditions (W/m^2)
S_{ref}	absorbed solar radiation at STC (W/m^2)
t	time (s)
$T(x,y,z)$	temperature field (K)
T_{amb}	Ambient temperature (K)
T_{cell}	PV cells temperature (K)
$T_{cell,ref}$	PV cells temperature at STC (K)
$T_{f,in}$	inlet water temperature (K)
$T_{front/rear}$	temperature of front or back surface (K)
T_{sky}	sky temperature (K)
$\boldsymbol{u}$	Fluid Velocity (m/s)
V	PV panel output voltage (V)
$V_{f,in}$	inlet water velocity (m/s)
$V_{pv,cell}$	volume of PV cells inside the module (m^3)

Greek symbols

α	absorptivity of PV cells
β	slope of PV panel
η_{pv}	electrical efficiency of PV panel
ε	turbulent dissipation rate (m^2/s^3)
$\varepsilon_{front,rear}$	emissivity of front glass or back sheet
ε_{ground}	emissivity of ground
ρ_{ground}	reflectivity of ground
ρ	density (kg/m^3)
θ	incidence angle of solar radiation
θ_r	refracted angle of solar radiation
σ_ε	Turbulent Prandtl number for ε
σ_k	turbulent Prandtl number for k
τ	transmitivity of top cover
$(\tau\alpha)$	transmitivity–Absorptivity product
μ	dynamic viscosity (Pa s)
μ_{isc}	temperature Coefficient of Short circuit current
μ_T	turbulent viscosity (Pa s)

experimental study to measure its performance. Othman et al. (2005) developed a double pass air-type PV/T collector with compound parabolic collectors (CPC) for solar concentration and fins for better heat transfer.

The performance prediction of PV panel needs radiation & optical model, thermal model and electrical model. The radiation & optical model (Klutcher, 1979; Perez et al., 1986; Reindl et al., 1990) is used to calculate the solar radiation absorbed in the PV cells. To estimate the electrical output of PV panels at a given operating condition, several electrical models have been reported in the literature (De Soto et al., 2006; Marion et al., 2004; King et al., 2004).

Thermal model is used to calculate temperature field in PV panel at given environmental and operating conditions. A substantial amount of research work on the development of thermal models either with cooling (Teo et al., 2011; Tiwari and Sodha, 2006a,b; Dubey and Tiwari, 2008; Dubey and Tiwari, 2009; Zondag et al., 2002) or without

cooling (Acciani et al., 2010; Jones and Underwood, 2001; King et al., 2004; Tina and Scrofani, 2008) has appeared in the literature. Tiwari and Sodha (2006a,b) developed an analytical model for the IPVTS collector and validated its performance against the experimental data of Huang et al. (2001). Their developed model for PV/T collectors was similar to the famous Hottel-Whillier model for flat-plate collectors (Hottel and Whillier, 1958). Dubey and Tiwari (2008) developed an analytical model for solar thermal collectors partially covered by PV cells. Using their model, they compared the performance of three design cases with varying fraction of PV cells covering the collector area. The result of their study showed that the improvement in instantaneous efficiency of the PV/T panel improved as the fraction of cell-covered area decreased. They later extended their model to calculate the performance in PV/T collectors in series and parallel combinations (Dubey and Tiwari, 2009). An improvement to the PV/T model by Dubey and Tiwari (2008) was suggested by Sarhaddi et al. (2010). They suggested that the accuracy of the model could be improved by using the equivalent electric circuit model to determine the electrical performance of the system and by using more detailed expressions for determining the thermal resistances within the system. Zondag et al. (2002) conducted an extensive study to study the effect of model complexity on prediction accuracy. Their findings suggested that the effect of including dynamical effects on a day's energy output prediction was very low, but the error in the steady state model increased for smaller periods of time.

Most of this reported research effort dealt with one-dimensional analytical thermal model for PV panels with temperature variation along the thickness only. Although simple 1D models are sufficiently accurate for long term performance predictions, more complex 2D and 3D models are needed to capture temperature gradient effect in PV/T collectors. Only such a model can handle complex flow patterns and design optimization tasks (Zondag et al., 2002).

In the present work, three dimensional numerical models have been developed to predict the thermal behavior of PV panels with and without cooling. The thermal models are coupled with radiation and electrical models to form a multi-physics model capable of calculating the thermal and electrical performance of the PV panels. The performance metric includes electrical power output, PV cell temperature and, in case of cooling, working fluid temperature at the outlet. Using this model, the effect of changing atmospheric and operating conditions on the performance of the PV system with and without cooling have been studied.

2. PV performance prediction model

Fig. 1 shows the flow chart of the performance prediction model used in this work. It has three physical models: radiation & optical, electrical and thermal. The models are sequentially coupled together to get the overall performance prediction. The external inputs required are the meteorological data and the PV site information. The outputs of the radiation and thermal models are input in the electrical model to calculate the power output. The following sections discuss the models in detail. In this study, the electrical model and the radiation and optical model were implemented in the MATLAB environment and the thermal model was implemented in ANSYS CFX environment.

2.1. Thermal model

The purpose of the thermal model is to calculate the three dimensional temperature distribution in the PV panel. The temperature distribution depends on the PV module materials, PV cell type, the panel configuration, the electrical load attached to the PV system, the prevailing environmental conditions and in case of cooling, the characteristics of the heat exchanger.

For a PV panel, the various modes of energy transfer in the PV panel are shown in Fig. 2. The panel gains energy by absorbing incoming solar radiation while energy is lost from it by convection and radiation to the environment, by energy transfer to the working fluid in the heat exchanger and in the form of electrical energy delivered to the electrical load. The amount of electrical energy taken out of the system depends on the load characteristics which determines the operating current–voltage (I–V) point and the electrical power output of the PV panel. Usually, maximum power point trackers are connected to the PV panel which ensure that panel operates near to the maximum power point on the I–V curve. In case of PV panel without cooling, the energy transfer to the heat exchanger through the PV panel back surface is replaced by convection and radiation losses to the environment.

2.1.1. Governing equations

The heat transfer in cooled PV panels involves a fluid and multiple solid domains. The fluid domain covers the working fluid inside the heat exchanger. There is a separate solid domain for each material layer (front cover, encapsulent, PV cells and back sheet) in the PV panel and for the heat exchanger body. Eqs. (1) and (2) are the heat transfer equations for solid and fluid domains respectively (Incropera and DeWitt, 1996).

$$\rho_i C_{p,i} \frac{\partial T_i(x,y,z)}{\partial t} = \nabla \cdot (\mathbf{q}_i) + Q_i \quad i = 1, 2, \ldots n \tag{1}$$

$$\rho C_p \frac{\partial T}{\partial t} + \rho C_p \mathbf{u} \cdot \nabla T(x,y,z) = \nabla \cdot (\mathbf{q}) + Q_{vh} \tag{2}$$

where

$$\mathbf{q} = k_{cond} \nabla T \tag{3}$$

and ρ is the density, C_p is the specific heat capacity, $T(x, y, z)$ is the temperature, t is the time, k_{cond} is the thermal conductivity, $\boldsymbol{q}$ is the heat transferred by conduction, Q is the internal heat generation, $\boldsymbol{u}$ is the fluid velocity and Q_{vh} is the viscous dissipation.

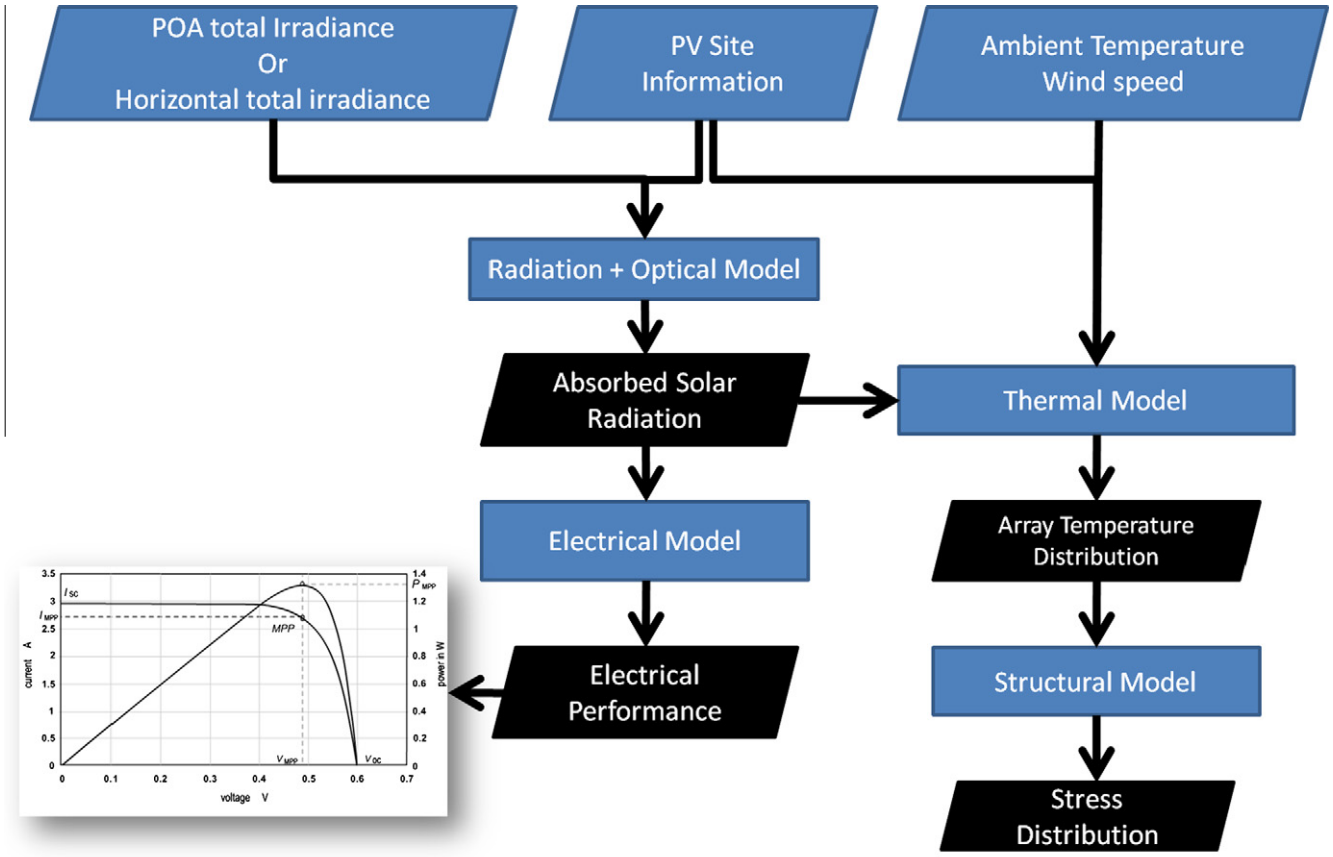

Fig. 1. Performance modeling of PV systems.

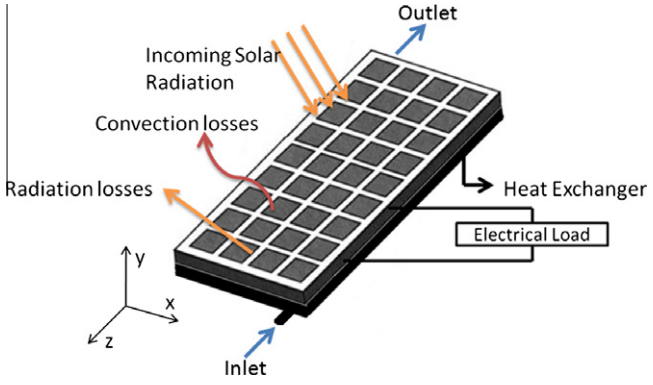

Fig. 2. Modes of energy transfer in a cooled PV panel.

The momentum and continuity equations governing the fluid flow inside the heat exchanger are given by Eqs. (4) and (5) (Wilcox, 1998).

$$\rho\frac{\partial \mathbf{u}}{\partial t}+\rho(\mathbf{u}\cdot\nabla)\mathbf{u}=\nabla\cdot\left[-p\mathbf{I}+(\mu+\mu_T)(\nabla\mathbf{u}+\nabla\mathbf{u}^T)-\frac{2}{3}\rho k\mathbf{I}\right] \tag{4}$$

$$\rho\nabla\cdot\mathbf{u}=0 \tag{5}$$

where p is the pressure, μ is the viscosity, μ_T is the turbulent viscosity and k is the turbulent kinetic energy. The turbulence model used is the k–ε model given by Eqs. (6)–(9) (Wilcox, 1998).

$$\rho\frac{\partial k}{\partial t}+\rho(\mathbf{u}\cdot\nabla)k=\nabla\cdot\left[\left(\mu+\frac{\mu_T}{\sigma_k}\right)\nabla k\right]+P_k-\rho\varepsilon \tag{6}$$

$$\rho\frac{\partial \varepsilon}{\partial t}+\rho(\mathbf{u}\cdot\nabla)\varepsilon=\nabla\cdot\left[\left(\mu+\frac{\mu_T}{\sigma_e}\right)\nabla\varepsilon\right]+C_{e1}\frac{\varepsilon}{k}P_k-C_{e2}\rho\frac{\varepsilon^2}{k} \tag{7}$$

$$\mu_T=\rho C_\mu\frac{k^2}{\varepsilon} \tag{8}$$

$$P_k=\mu_T[\nabla\mathbf{u}:(\nabla\mathbf{u}+(\nabla\mathbf{u})^T)] \tag{9}$$

where P_k is production term and ε is the turbulent dissipation rate. The values of the model constants are $C_\mu=0.09$, $C_{\varepsilon1}=1.44$, $C_{\varepsilon2}=1.92$, $\sigma_k=1.0$ and $\sigma_\varepsilon=1.3$ (Wilcox, 1998).

2.1.2. Thermal load and boundary conditions

The incoming solar radiation is used to calculate the absorbed solar radiation using the radiation and optical model. (Reindl et al., 1990; Duffie and Beckman, 2006). The model is defined by the following equation:

$$\frac{S}{S_{ref}}=M\frac{G_b+A_iG_d}{G_{ref}}R_{beam}K_{\tau\alpha,b}+M\frac{(1-A_i)G_d}{G_{ref}}K_{\tau\alpha,d}\left(\frac{1+\cos\beta}{2}\right)\times\left(1+f\sin^3\left(\frac{\beta}{2}\right)\right)+M\frac{G}{G_{ref}}\rho_{ground}K_{\tau\alpha,g}\left(\frac{1-\cos\beta}{2}\right) \tag{10}$$

where

$$S_{ref}=(\tau\alpha)_nG_{ref} \tag{11}$$

and S is the absorbed solar radiation, G is the horizontal plane solar radiation, R_{beam} is the ratio of beam radiation on tilted plane to that on horizontal plane, ρ is the reflectivity of the ground, β is the tilt angle of the PV panels, the factor A_i is the Anisotropy index and M is the air mass modifier. The subscripts b, d, g and ref represent the beam, diffuse, ground reflected and reference solar radiations respectively and n represents a zero incidence angle. The incidence angle modifiers $K_{\tau\alpha}$ for the beam, diffuse and ground-reflected radiation components are defined by the following equation:

$$K_{\tau\alpha} = \frac{(\tau\alpha)}{(\tau\alpha)_n} \tag{12}$$

The absorptivity α of the PV cells is taken as 0.9 (Tiwari and Sodha, 2006a,b; Notton et al., 2005) and transmitivity of the front glass cover is defined by Eq. (13) (De Soto et al., 2006).

$$\tau(\theta) = e^{-\left(KL_{glass}/\cos\theta_r\right)}\left[1 - \frac{1}{2}\left(\frac{\sin^2(\theta_r-\theta)}{\sin^2(\theta_r+\theta)} + \frac{\tan^2(\theta_r-\theta)}{\tan^2(\theta_r+\theta)}\right)\right] \tag{13}$$

where τ is the transmitivity, K is the extinct coefficient and L_{glass} is the thickness of the front cover. θ and θ_r are the angles of incidence and refraction.

A portion of the absorbed solar radiation is converted to electrical energy while the remaining energy raises the temperature of the PV panel. The absorbed solar radiation is applied to the heat transfer equation of the PV cell layer as an internal heat generation, Q, which is calculated using the following equation:

$$Q = \frac{(1-\eta_{pv}) \times S \times A_{panel}}{V_{pv,cell}} \tag{14}$$

where η_{pv} is the electrical efficiency of the PV panel, A_{panel} is the front area of the PV panel and the $V_{pv,cell}$ is the volume of the PV cells in the panel.

Convection and radiation boundary conditions were applied to the PV panel top and bottom surfaces for the case without cooling and to the top surface only for the case with cooling in the form of an equivalent heat loss coefficient which was calculated using the following equation:

$$h = h_{conv,forced} + h_{conv,free} + h_{radiation} \tag{15}$$

where h is the equivalent heat loss coefficient. $h_{conv,forced}$, $h_{conv,free}$ and $h_{radiation}$ for the front and rear sides are calculated iteratively using Eq. (16) by Sparrow et al. (1979), Eq. (17) by Lloyd and Moran (1974) and Eq. (18) by Duffie and Beckman (2006) respectively.

$$Nu = 0.86Re^{1/2}Pr^{1/3} \tag{16}$$

$$Nu = \begin{cases} 0.76Ra^{1/4} & \text{for} \quad 10^4 < Ra < 10^7 \\ 0.15Ra^{1/3} & \text{for} \quad 10^7 < Ra < 3\times10^{10} \end{cases} \tag{17}$$

$$h_{radiation}(T_{front/rear} - T_{amb}) = \varepsilon_{front/rear}F_{front/rear-sky}\sigma(T^4_{front/rear} - T_{sky^4}) + \frac{\sigma F_{front/rear-ground}(T^4_{front/rear} - T_{ground})}{\frac{1}{\varepsilon_{front/rear}} + \frac{1}{\varepsilon_{ground}} - 1} \tag{18}$$

where Nu is the Nusselt's number, Re is the Reynolds's number, Pr is the Prandl's number, Ra is the Raleigh's number, ε is the emissivity, F is the geometric factor and σ is the Stefan–Boltzmann's constant. T_{sky} was taken as T_{amb} −20 K (Jones and Underwood, 2001) and the ground temperature was assumed to be equal to the ambient temperature (Armstrong and Hurley, 2010).

The corresponding boundary conditions applied to the heat transfer equations of top and bottom layers of the PV panel is given by the following equation:

$$-\mathbf{n}\cdot\mathbf{q} = h(T_{amb} - T_{front/rear}) \tag{19}$$

where $\mathbf{n}$ is the surface normal and T_{amb} and T_s are the ambient and surface temperatures.

For the fluid domain, the inlet boundary conditions were defined by the inlet water temperature, $T_{f,in}$ and a uniform velocity, $V_{f,in}$ as expressed by the following equations:

$$T = T_{f,in} \tag{20}$$

$$\mathbf{u} = -\mathbf{n}V_{f,in} \tag{21}$$

The outlet condition is set to zero gauge pressure and no slip condition is applied to all internal surfaces of the heat exchanger. A perfect contact is assumed between all the layers in the PV panel.

2.1.3. Implementation of the thermal model

The thermal model was implemented in *ANSYS CFX* environment as a computation fluid dynamics (*CFD*) model of the PV panel with and without a heat exchanger attached to its back. The working fluid in the heat exchanger was assumed to be water. The geometric model is 3-dimensional and was prepared and meshed using *ANSYS*

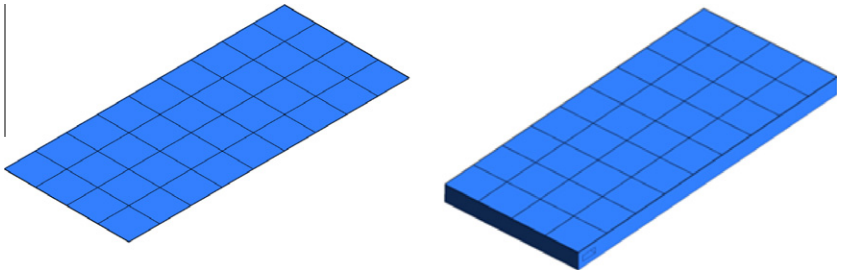

Fig. 3. Geometry of thermal models with and without cooling.

Table 1
Material properties used in thermal model.

Material	Layer	Thermal conductivity (W/m K)	Specific heat capacity (J/kg K)	Density (kg/m^3)
Silicon	Solar cell	130	677	2330
Tempered glass	Top cover	2	500	2450
Polyester	Bottom cover	0.15	1250	1200
Ethyl vinyl acetate	Encapsulent	0.311	2090	950
Aluminum	Heat exchanger	237	903	2702

Mechanical code. The geometry of the model without and with cooling is shown in Fig. 3. The heat exchanger design selected for this study was the parallel channel type heat exchanger. The model consists of four solid domains for the PV panel: front cover, back sheet, encapsulent and the PV cells and two domains for the heat exchanger: a solid domain for the heat exchanger body and a fluid domain for the water inside the heat exchanger. The thermal properties for the various material used in the model are given in Table 1.

2.2. Electrical model

The electrical model used in the present work is a newly developed 7 parameters model (Siddiqui, 2011) in which a PV device is represented by an equivalent electric circuit of Fig. 4 (Duffie and Beckman, 1991) and the current–voltage relationship for the PV devices is governed by the following equation:

$$I = I_L - I_o\left(exp\left(\frac{V + I\cdot R_s}{a}\right) - 1\right) - \frac{V + I\cdot R_s}{R_{sh}} \tag{22}$$

To use the model, the parameters I_L, I_o, a, R_s and R_{sh} are first determined at a reference condition and then translated to the operating condition using the translation Eqs. (23)–(27). The parameters m and n are determined using two additional maximum power values at a higher temperature and a lower irradiance.

$$a = a_{ref}\left(T_{cell}/T_{cell,ref}\right)^n \tag{23}$$

$$I_L = (S/S_{ref})^m(I_{L,ref} + \mu_{isc}(T_{cell} - T_{cell,ref})) \tag{24}$$

$$I_o = I_{o,ref}\left(T_{cell}/T_{cell,ref}\right)^3 e^{\left(\frac{NCS.T_{cell,ref}}{a_{ref}}\left(E_{g,ref}/T_{cell,ref} - E_g/T_{cell}\right)\right)} \tag{25}$$

$$R_{sh} = \frac{S_{ref}}{S}R_{sh,ref} \tag{26}$$

$$R_s = R_{s,ref} \tag{27}$$

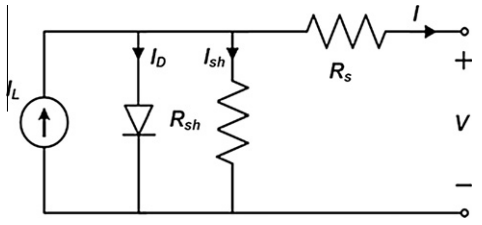

Fig. 4. Equivalent circuit of an actual PV cell.

3. Model validation

To validate the current thermal model, three types of validations were carried out. For the thermal model without cooling, two validations were done, one against experimentally measured data and second against the normal operating conditions temperature (NOCT) reported in the module datasheet. The model for PV panel with cooling was validated against a simplified one dimensional model. The details of the validations are presented in the following sections.

3.1. Validation of thermal model without cooling using manufacturer data

Using the thermal model for PV panels without cooling, the normal operating conditions temperature (*NOCT*) of AstroPower AP-110 mono crystalline silicon PV module was predicted and compared to the value provided in the module datasheet. The inputs to the model were an incident solar radiation of 800 W/m^2, an ambient temperature of 20 °C, and a wind speed of 1 m/s on the front surface. The NOCT reported in the datasheet of the module is 45 °C. The predicted value from the model, shown in Fig. 5, is 43.3 °C (316.3 K). This represents a 3.78% error in PV cell temperature prediction.

3.2. Validation of thermal model without cooling using experimental data

The thermal model for PV panel without cooling was validated using experimentally measured data for a 5940 W PV site using Schott Solar SAPC-165 multicrystalline silicon PV panel. The site is located in Tallahassee, Florida, USA. The data recorded at the site included plane-of-array incident solar radiation, ambient temperature, PV panel back-surface temperature and electrical current, voltage and power. The meteorological data for the PV site for one day (May 15, 2005) was taken from the PV performance database maintained by *Florida Solar Energy Center* and is shown in Fig. 6 (Florida Solar Energy Center PV performance database). The wind speed data which was not measured at the site was taken from the measurements made at Tallahassee regional airport (Wolfram Mathematica Weather Data). The wind speed data is shown in Fig. 7. The developed model was used

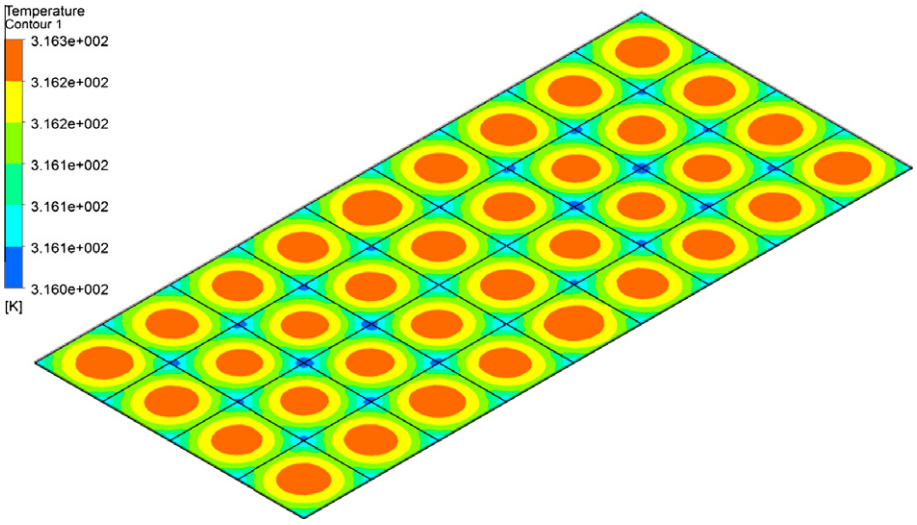

Fig. 5. Model validation for thermal model without cooling using manufacturer data.

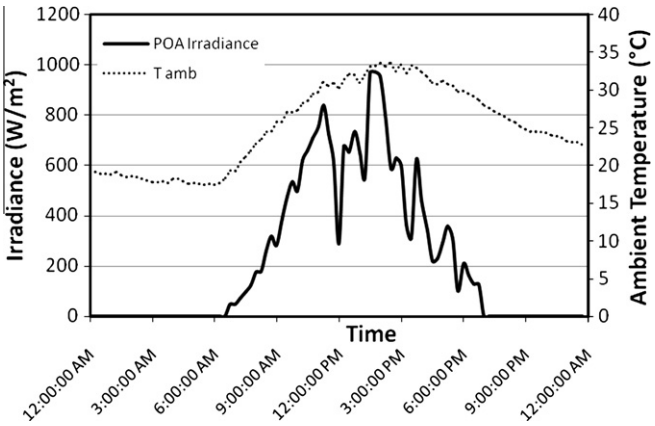

Fig. 6. Irradiance and ambient temperature data for the PV Site (Florida Solar Energy Center PV performance database).

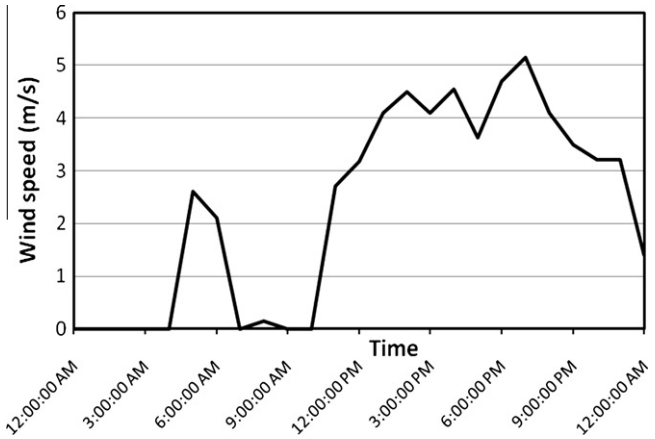

Fig. 7. Wind speed data for Tallahassee, Florida on May 15, 2005 (Wolfram Mathematica Weather Data).

to calculate the transient thermal response of the PV panel for the environmental conditions for the selected day and

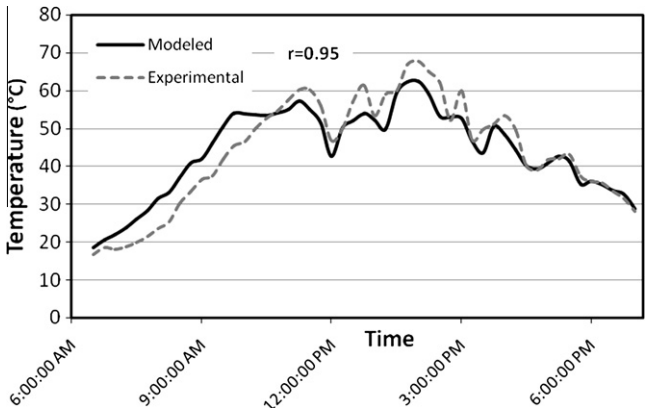

Fig. 8. Model validation for thermal model without cooling using experimental data.

the module back surface temperature predicted by the current model was compared to the experimentally measured values. The comparison is shown in Fig. 8. The root mean square error in the model prediction of panel back surface temperature was 4.9 °C. The correlation factor (r) was calculated to be 0.95. It is important to note here that the error in the temperature prediction incorporates the error in the radiation model as well the errors in the measurements of irradiance, ambient temperature, wind speed as well the measured panel back surface temperature.

3.3. Validation of thermal model with cooling using analytical model

To validate the thermal model with cooling, the results of the model for the simple case of parallel channel heat exchanger attached to an AstroPower AP-110 module were compared with the analytical model for the parallel channel heat exchanger PV/T collector presented by Sarhaddi et al. (2010). Temperatures of the fluid outlet and PV cells

Table 2
Model validation for thermal model with cooling.

Inlet velocity (m/s)	Cell temperature (°C)		Outlet fluid temperature (°C)	
	Current model	Using Sarhaddi et al. (2010)	Current model	Using Sarhaddi et al. (2010)
0.1	30.6	29.1	25.7	25.6
0.05	32.5	31.5	26.5	26.1
0.01	41.1	39.8	30.7	26.3

were compared at various inlet velocities. The results of the comparison are shown in Table 2. The root mean square errors in the prediction of PV cells and outlet fluid temperatures were 0.74 °C and 1.47 °C respectively.

4. Results and discussion

Using the developed and validated model, a study was conducted to see the effect and usefulness of cooling on the performance of the PV panel under different atmospheric and operating conditions. The effect of atmospheric factors such as ambient temperature and solar irradiance on the performance (T_{cell}, $T_{water,out}$, η_{pv}, *Electric Power*) of PV panels with and without cooling were studied. Additionally, the effect of heat exchanger inlet conditions and thermal contact resistance between the PV panel and heat exchanger on the performance of cooled PV panels was also analyzed.

In all of the following studies, a standard case was studied by varying only a single parameter. The PV module selected for the study was AstroPower AP-110 module. The electrical model reference parameters for the selected module at *STC* are given in Table 3.

The operating and environmental conditions considered for the standard case were 800 W/m^2 absorbed radiation, 25 °C ambient temperature and for cooling, inlet water velocity and temperature equal to 0.05 m/s and 25 °C. A perfect contact was assumed between the PV panel and the heat exchanger. Fig. 9 shows the temperature distribution in PV cells for the panels without cooling and with cooling for the standard case. It can be seen that in the panel without cooling, no appreciable temperature gradient exists while in the panel with cooling, there is almost a 4 °C temperature difference in PV cells across the panel. This difference is due to the non-uniform water flow in the heat exchanger. Such temperature profiles cannot be determined by simple 1-D models such as the ones presented by Tiwari and Sodha (2006a,b) and Sarhaddi et al. (2010).

Table 3
Electrical model reference parameters for the selected PV module.

Parameter	Value
$I_{L,ref}$	7.5084 A
$I_{o,ref}$	3.4686×10^{-6} A
a_{ref}	1.4249 V^{-1}
$R_{s,ref}$	0.0527 Ω
$R_{sh,ref}$	46.8713 Ω
m	1.0959
n	1.1368

4.1. Effect of absorbed solar radiation on panel performance

Incident solar radiation is one of the most important environmental parameters that determine the performance of PV panels. In order to study the effect of cooling on the performance of PV panels under different amounts of solar radiation, the developed models for PV panels with cooling and without cooling were used to calculate the PV cells and water outlet temperatures, electrical efficiency and electrical power output of the panel for different amounts of absorbed radiation. The selected range of absorbed radiation was taken from 200 W/m^2 to 1000 W/m^2. The results are shown in Fig. 10. The average PV cell temperature for the PV panel without cooling ranges from 33.7 °C to 62.1 °C whereas for the panel with cooling, the range is from 26.9 °C to 34.4 °C. The outlet water temperature ranges from 25.4 °C to 26.4 °C which is not very high. The electrical efficiency of the PV panel without cooling dropped from 7.8% at 200 W/m^2 to 7.43% at 1000 W/m^2 while for the panel with cooling, the efficiency increased from 8.47% to 10.55%. This increase in the panel efficiency was due to the increase in irradiance. A slight increase in efficiency was also noticed for the panel without cooling with the increase in absorbed radiation from 200 W/m^2 to 400 W/m^2 but as the PV cell temperature increased, its effect became dominant and the efficiency began to drop. The different variations in efficiency for the cooled and uncooled panels also translated to the electric power outputs of the two panels where it resulted in a better improvement in system performance at higher irradiances. The difference in the power output of the cooled and uncooled panels at 200 W/m^2 was only 1.5 W and increased to 35.7 W for 1000 W/m^2.

4.2. Effect of ambient temperature on panel performance

Ambient temperature is another important environmental factor that affects PV performance. In order to study the effect of cooling on PV panel performance working in different ambient temperatures, the developed models were used to calculate the PV cells and water outlet temperatures, electrical efficiency and electrical power output of the PV panel with and without cooling for ambient temperatures ranging from 0 °C to 50 °C. This range of ambient temperatures covers PV panels working in cold winter conditions to very hot summer conditions. The results are shown in Fig. 11. The cooled PV panel showed no significant performance variation for the entire ambient temperature range. On the other hand, for the PV panel without cooling, the average PV cell temperature increased from 31.5 °C to 79.3 °C as ambient temperature increases from 0 °C to 50 °C, the electrical efficiency drops from 10.46% to 5.16%,

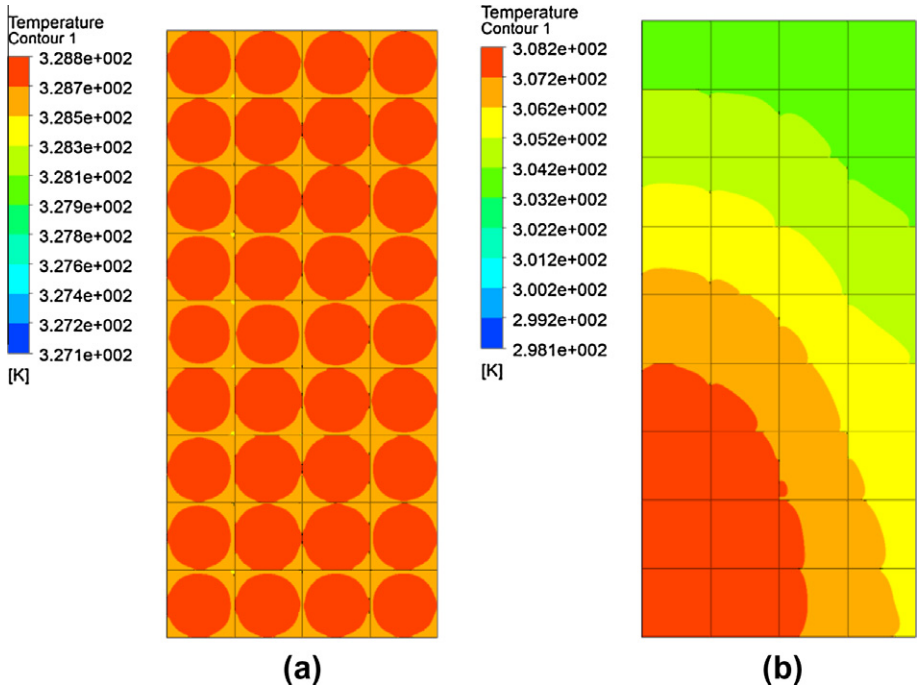

Fig. 9. Temperature distribution in PV cells for panel (a) without cooling (b) with cooling.

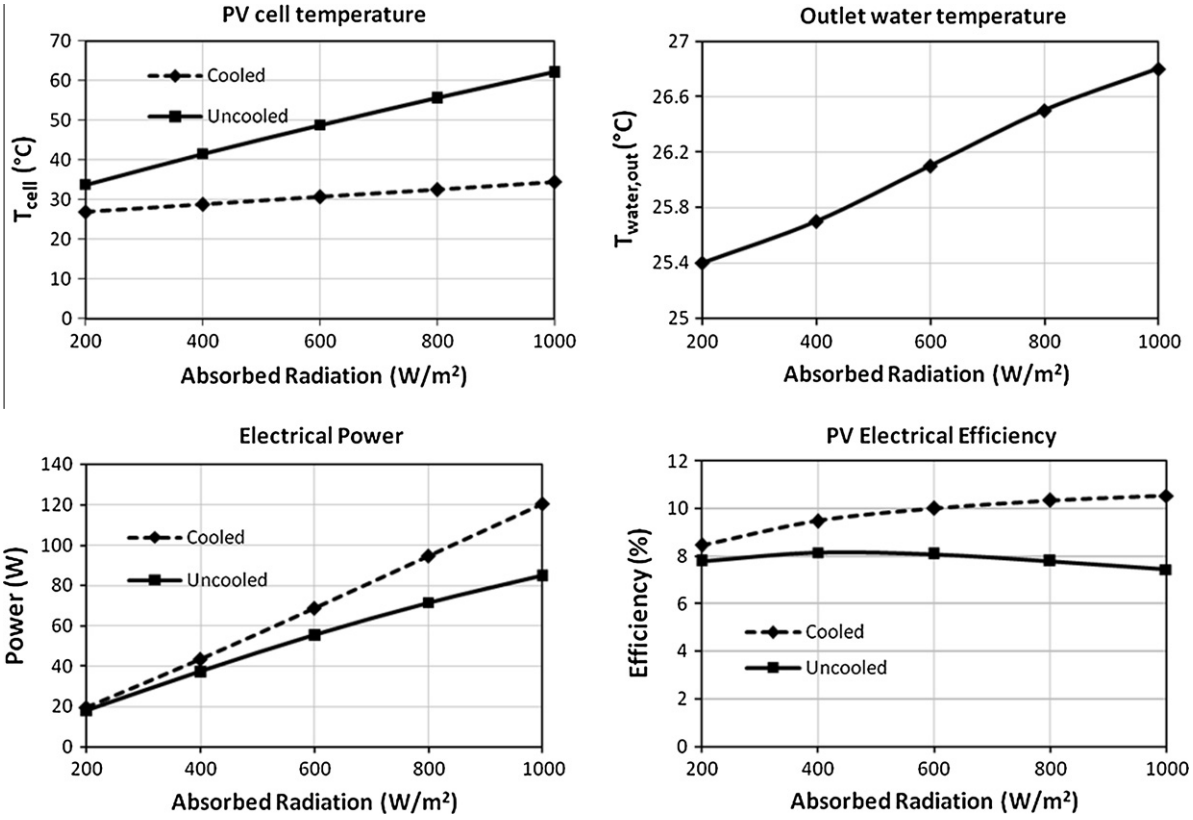

Fig. 10. PV panel performance variation with absorbed radiation. ($T_{amb} = 25$ °C, $V_{f,in} = 0.05$ m/s, $T_{f,in} = 25$ °C).

the electrical power output decreases from 95.7 W to 47.2 W. This represents a 50.7% decrease in electrical power output for the PV panel without cooling from the coldest to the hottest environment considered. On the other hand, the electric power output for the cooled panel showed only a 5.5 W drop.

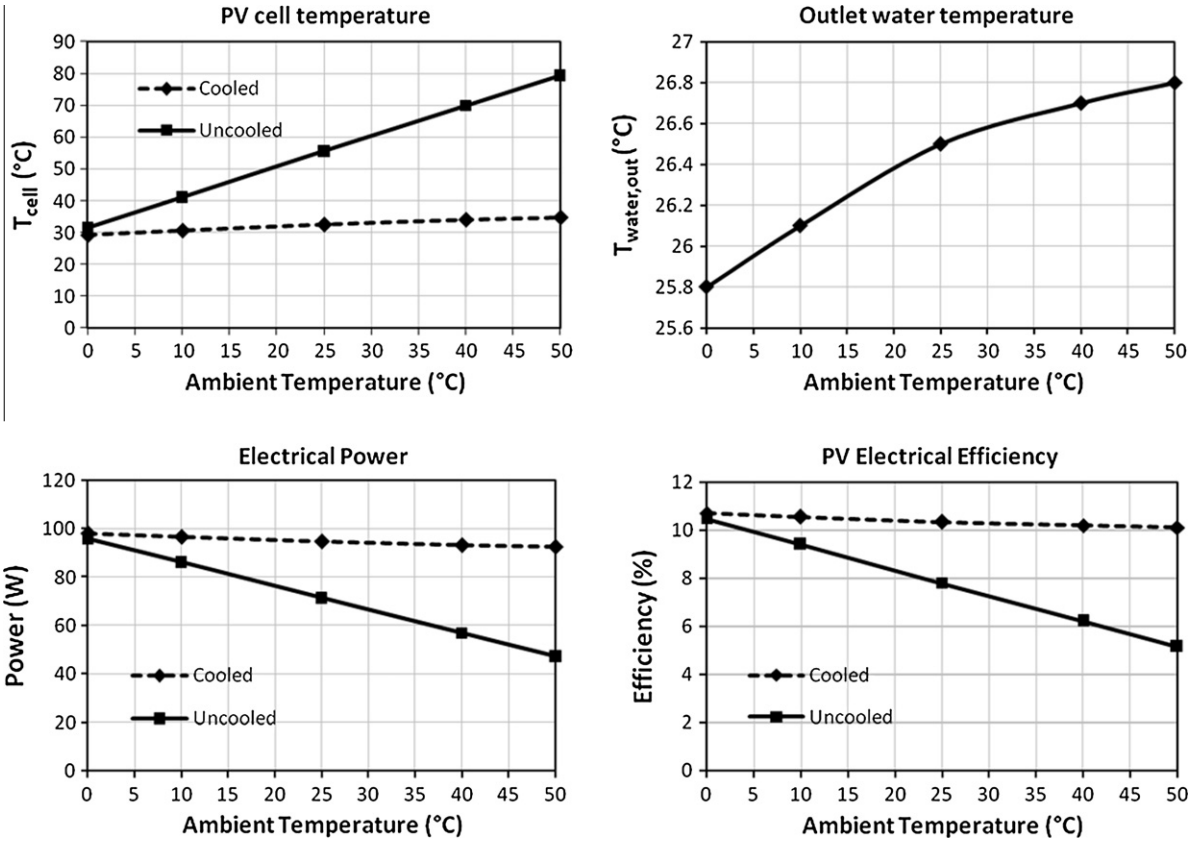

Fig. 11. PV panel performance variation with ambient temperature. ($S = 800$ W/m^2, $V_{f,in} = 0.5$ m/s, $T_{f,in} = 25$ °C).

4.3. Effect of heat exchanger inlet conditions

The operating parameters of the heat exchanger also affect the performance of the PV panel. In this study, the effect on performance of heat exchanger parameters, inlet velocity and inlet temperature, were studied. Fig. 12 shows the results for inlet velocity variation. The range of inlet velocities was taken from 0.01 m/s to 0.1 m/s. For this range, the average PV cell temperature decreased from 41.1 °C to 30.6 °C and the outlet water temperature dropped from 30.7 °C to 25.7 °C. The increase in electrical efficiency for this range was 10 W.

Fig. 13 shows the variation in the PV panel performance with inlet temperature variation. The range selected for inlet water temperature variation was 5–45 °C. Such high inlet temperatures can also result when the heat exchangers of multiple PV panels are connected in series. For the selected range of inlet temperatures, the average PV cell temperatures increase from 14.5 °C to 50.1 °C, the efficiency drops from 12.28% to 8.4% and this causes the elec-

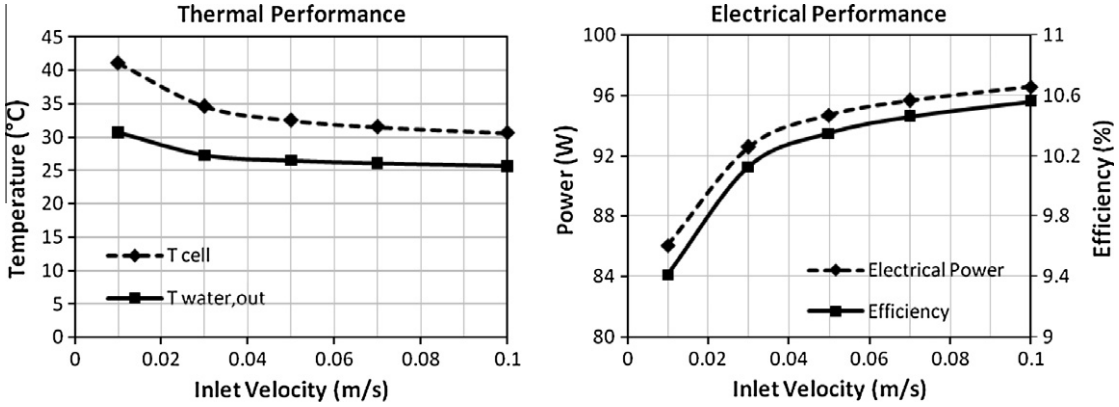

Fig. 12. PV panel performance variation with heat exchanger inlet velocity. ($S = 800$ W/m^2, $T_{amb} = 25$ °C, $T_{f,in} = 25$ °C).

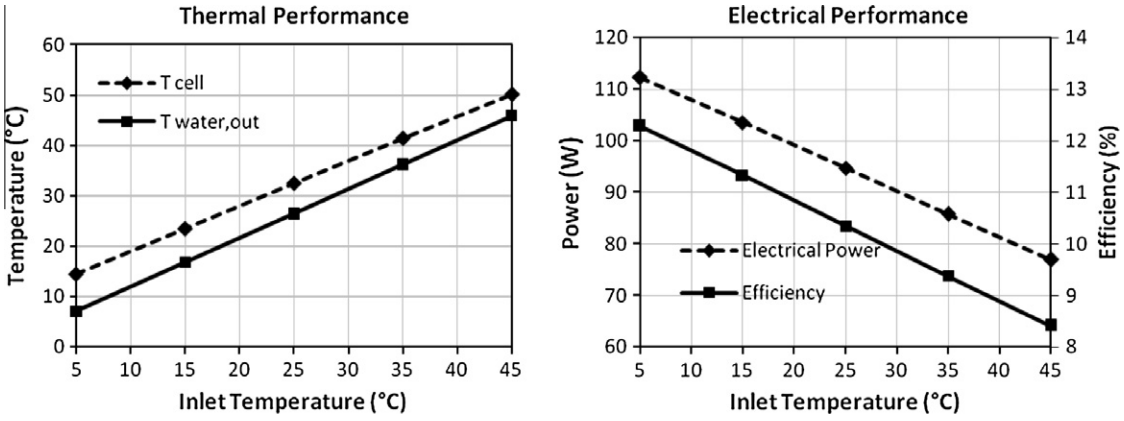

Fig. 13. PV panel performance variation with heat exchanger inlet temperature. ($S = 800$ W/m^2, $T_{amb} = 25$ °C, $V_{f,in} = 0.5$ m/s).

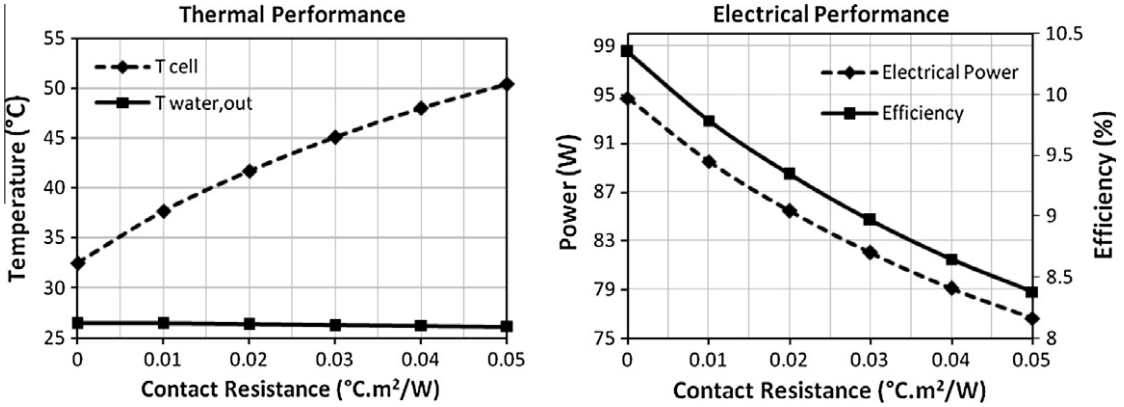

Fig. 14. PV panel performance variation with change in thermal contact resistance. ($S = 800$ W/m^2, $T_{amb} = 25$ °C, $V_{f,in} = 0.5$ m/s, $T_{f,in} = 25$ °C).

trical power output of the PV panel to drop by almost 35 W.

4.4. Effect of thermal contact resistance

Inefficient thermal contact between the PV panel and the heat exchanger can also lead to degradation of PV panel performance. The range of thermal contact resistance used in this study was 0.005–0.05 °C m^2/W and was taken from the work of Bahrami et al. (2006). Fig. 14 shows the results of the study. From the case of ideal contact to the case of maximum contact resistance considered, the increase in PV cell temperature was around 18 °C. The absolute drop in efficiency was around 2% and about 19% of electrical power was lost due to the contact resistance.

5. Conclusions

A three dimensional numerical model to predict thermal and electrical performance of the PV panel for given environmental and operating conditions is presented and validated in this paper. From the various studies conducted using this model, the following conclusions were drawn:

- Within the absorbed radiation range of 200–1000 W/m^2 at an ambient temperature of 25 °C, PV panel with cooling showed an improvement in its efficiency from 8.47% to 10.5% with almost linearly increasing electrical power from 17.8 W to 120 W. Whereas, for the same range, efficiency reduces from 7.8% to 7.4% for panel without any cooling.
- For an absorbed radiation of 800 W/m^2 and an increase in ambient temperature from 0 °C to 50 °C, the efficiency and electrical power of PV panel with cooling showed a very small decrease from 10.7% to 10.1% and 98 W to 92.5 W, respectively. For PV panel without cooling, the electrical power output decreases from 95.7 W to 47.2 W under the same temperature range.
- It was shown that the thermal contact resistance between PV panel and heat exchanger can result in significant power loss due to higher PV cell temperatures. The decrease in electrical power output of the panel with contact resistance equal of 0.05 °C m^2/W was around 19% with respect to panel having no thermal resistance.
- The results of the conducted studies show that the effect of cooling will be more pronounced in environments like the Middle East having high solar irradiance and ambient temperature.

Acknowledgments

The authors would like to acknowledge the support of King Fahd University of Petroleum and Minerals through the Center for Clean Water and Clean Energy at KFUPM (DSR project # R6-DMN-08) and MIT. The authors would also like to thank Prof. S.M. Zubair and Prof. Anwar K. Sheikh for their helpful comments during the development of this work.

References

Acciani, G., Falcone, O., Vergura, S., 2010. Analysis of the thermal heating of poly-Si and a-Si photovoltaic cell by means of FEM. In: In International Conference on Renewable Energies and Power Quality.

Armstrong, S., Hurley, W.G., 2010. A thermal model for photovoltaic panels under varying atmospheric conditions. Applied Thermal Engineering 30 (11–12), 1488–1495.

Bahrami, M., Yovanovich, M.M., Marotta, E.E., 2006. Thermal joint resistance of polymer-metal rough interfaces. Journal of Electronic Packaging 128 (1), 23–29.

De Soto, W., Klein, S.A., Beckman, W.A., 2006. Improvement and validation of a model for photovoltaic array performance. Solar Energy 80 (1), 78–88.

Dubey, S., Tiwari, G.N., 2008. Thermal modeling of a combined system of photovoltaic thermal (PV/T) solar water heater. Solar Energy 82 (7), 602–612.

Dubey, S., Tiwari, G.N., 2009. Analysis of PV/T flat plate water collectors connected in series. Solar Energy 83 (9), 1485–1498.

Duffie, J.A., Beckman, W.A., 1991. Solar Engineering of thermal processes, second ed. John Wiley & Sons, Inc., New York.

Duffie, J.A., Beckman, W.A., 2006. Solar Engineering of thermal processes, third ed. John Wiley & Sons, Inc., Hoboken, New Jersey.

Florida Solar Energy Center PV Performance Database. <http://www.logger.fsec.ucf.edu/cgi-bin/wg40.exe?user=pvgroup> (accessed 10.11.2010).

Hottel, H.C., Whillier, A., 1958. Evaluation of flat-plate solar-collector performance. Transactions of the Conference on Use of Solar Energy 2 (1), 74.

Huang, B.J., Lin, T.H., Hung, W.C., 2001. Performance evaluation of solar photovoltaic / thermal systems. Solar Energy 70 (5), 443–448.

Incropera, F.P., DeWitt, D.P., 1996. Fundamentals of Heat and Mass Transfer, fourth ed. John Wiley & Sons, Inc.

Jones, A.D., Underwood, C.P., 2001. A thermal model for photovoltaic systems. Solar Energy 70 (4), 349–359.

King, D.L., Boyson, W.E., Kratochvil, J.A., 2004. Photovoltaic Array Performance Model. Sandia National Labs report, Albuquerque, New Mexico.

Klutcher, T.M., 1979. Evaluation of models to predict insolation on tilted surfaces. Solar Energy 23 (2), 111–114.

Lloyd, J.R., Moran, W.P., 1974. Natural convection adjacent to horizontal surface of various planforms. ASME Journal of Heat Transfer 96 (4), 443–451.

Marion, B., Rummel, S., Anderberg, A., 2004. Current-voltage curve translation by bilinear interpolation. Progress in Photovoltaics: Research and Applications 12 (8), 593–607.

Notton, G., Cristofari, C., Mattei, M., Poggi, P., 2005. Modelling of a double-glass photovoltaic module using finite differences. Applied Thermal Engineering 25 (17–18), 2854–2877.

Othman, M.Y.H., Yatim, B., Sopian, K., Abu Bakar, M., 2005. Performance analysis of a double-pass photovoltaic/thermal (PV/T) solar collector with CPC and fins. Renewable Energy 30 (13), 2005–2017.

Perez, R., Stewart, R., Arbogast, C., Seals, R., Scott, J., 1986. An anisotropic hourly diffuse radiation model for sloping surfaces: description, performance validation, site dependency evaluation. Solar Energy 36 (6), 481–497.

Reindl, D.T., Beckman, W.A., Duffie, J.A., 1990. Evaluation of hourly tilted surface radiation models. Solar Energy 45 (1), 9–17.

Sarhaddi, F., Farahat, S., Ajam, H., Behzadmehr, A., Adeli, M.M., 2010. An improved thermal and electrical model for a solar photovoltaic thermal (PV/T) air collector. Applied Energy 87 (7), 2328–2339.

Siddiqui, M.U., 2011. Multiphysics modeling of Photovoltaic panels and Arrays with auxiliary thermal collectors. MS Thesis, King Fahd University of Petroleum & Minerals, Saudi Arabia.

Skoplaki, E., Palyvos, J.A., 2009. On the temperature dependence of photovoltaic module electrical performance. A review of efficiency/power correlations. Solar Energy 83 (5), 614–624.

Sparrow, E.M., Ramsey, J.W., Mass, E.A., 1979. Effect of finite width on heat transfer and fluid flow about an inclined rectangular plane. ASME Journal of Heat Transfer 101, 199–204.

Teo, H.G., Lee, P.S., Hawlader, M.N.A., 2011. An active cooling system for photovoltaic modules. Applied Energy 90 (1), 309–315.

Tina, G.M., Scrofani, S., 2008. Electrical and thermal model for PV module temperature evaluation. In: Electrotechnical Conference, 2008. MELECON 2008. The 14th IEEE Mediterranean. pp. 585–590.

Tiwari, A., Sodha, M., 2006a. Performance evaluation of hybrid PV/thermal water/air heating system: a parametric study. Renewable Energy 31 (15), 2460–2474.

Tiwari, A., Sodha, M.S., 2006b. Performance evaluation of solar PV/T system: an experimental validation. Solar Energy 80 (7), 751–759.

Wilcox, D.C., 1998. Turbulence Modeling for CFD, second ed. DCW Industries.

Wolfram Mathematica Weather Data. <http://www.wolframalpha.com/input/?i=wind+speed+tallahassee+florida+may+15+2005> (accessed 28.09.2011).

Zondag, H.A., de Vries, D.W., van Helden, W.G.J., van Zolingen, R.J.C., van Steenhoven, A.A., 2002. The thermal and electrical yield of a PV-thermal collector. Solar Energy 72 (2), 113–128.